

1 **Biaxial bending of SFRC slabs:**
2 **is conventional reinforcement necessary?**

3 Marco di Prisco, Matteo Colombo, Ali Pourzarabi
4

5 **ABSTRACT**

6 Fibre reinforced concrete shows enhanced performance in statistically redundant bi-dimensional
7 structural elements that undergo biaxial bending. However, the lack of reinforcing rebars in fibre
8 reinforced structural elements may affect the structural ductility which may further affect the
9 overall load bearing capacity of these structures. To investigate the influence of fibres in such
10 elements, six concrete plates of 2000×2000×150 mm reinforced with steel fibres and/or reinforcing
11 rebars are tested under a central concentrated load. Two of the elements are reinforced with only 35
12 kg/m³ of steel fibres, two are reinforced with 2-way conventional reinforcing rebars (35 kg/m³, in
13 each direction) and two are reinforced with both steel fibres and rebars. The specimens are simply
14 supported at the middle of each side by means of a bilateral restraint: the deflection response and
15 cracking behaviour of all the specimens are recorded and compared. Moreover, the methodology
16 introduced in the *fib* Model Code 2010 for design of steel fibre reinforced concrete is implemented
17 to predict the ultimate load bearing capacity of these elements and its reliability is determined in
18 comparison with the experimental values. The comparison of the behaviour of the specimens
19 reinforced only with steel fibres, with those reinforced with steel rebars, shows the higher efficiency
20 of steel fibres in terms of load carrying capacity, counterbalanced by a lower ductility. The
21 combination of steel fibres and rebars allows for a better exploitation of the capacity of both
22 reinforcement solutions. Finally, the reliability of the approach implemented for the ultimate load
23 prediction is shown and the need of rebars in providing ductility in fibre reinforced concrete
24 members is underlined.

25 **Keywords:** biaxial bending, reinforcement efficiency, fibre reinforced concrete, slabs,
26 serviceability and ultimate behaviour, ductility

27 **1. INTRODUCTION**

28 The addition of steel fibres in concrete to prevent the brittle tensile behaviour shown by plain
29 concrete has been studied for over half a century after the observation of the crack arrest mechanism
30 by Romualdi and Batson [1]. As early as 1971, Shah and Rangan [2] pointed out the effect of fibres
31 in tensile, flexural, and compressive behaviour of steel fibre reinforced concrete (SFRC) and also
32 briefly studied some related aspects like fibre volume, geometry, and orientation on tensile
33 behaviour of concrete. Ever since, different properties and influencing factors of this material have
34 been extensively studied [3]–[6].

35 Steel fibres are commonly adopted as a substitution for diffused reinforcement in concrete
36 structures. Fibre addition to reinforced concrete members is an effective solution for cracking
37 control leading to more durable structures [7]. While in a conventionally reinforced concrete
38 member tensile stresses are transferred to concrete out of the cracks by stretched rebars through the
39 steel-concrete bond, in fibre reinforced concrete (FRC) due to the presence of fibres, concrete is
40 able to carry tensile stresses also along the cracks. This stiffening effect brought by fibres is
41 responsible for closer crack spacing and narrower crack widths in a structural system containing
42 both reinforcing bars and fibres (R/FRC) [8]–[12].

43 There are several studies in the literature concerning the simultaneous application of reinforcing
44 bars and fibres in simply supported beams and slabs under a three-point or four-point bending test.
45 Meda et al. [13] tested concrete beams of 2000 mm long in a four-point bending setup. The
46 incorporation of 30 kg/m^3 and 60 kg/m^3 of steel fibres reduced deflections for respectively 7% and
47 25% in the SLS range of behaviour. Comparable results are reported by Oh [14] and Alsayed [15].
48 Vandewalle [16] studied the effect of fibre volume and aspect ratio on crack spacing in fibre
49 reinforced R/C beams and proposed a relationship to take into account the reduced crack spacing in

50 R/C beams incorporating fibres. The same testing method was adopted by Tan et al. [17] to examine
51 short term and long term flexural cracking behaviour of R/FRC beams. A dosage of up to 2% of
52 steel fibres with an interval of 0.5% volume was investigated in the beams. While primary cracks
53 appeared at the location of stirrups, maximum crack width reduced with fibre dosage at all loading
54 stages for an instantaneous deflection and also for long term flexural creep testing. Mertol et al. [18]
55 tested lightly and heavily reinforced concrete beams with and without fibres and pointed out the
56 effect of fibres in reducing ductility in very low reinforcement ratios. In a work by Pujadas et al.
57 [19] concrete slabs of 3000×1000×200 mm were tested in a four-point bending configuration with
58 addition of 0.25% and 0.5% by volume of steel and polypropylene fibres. Steel fibres were effective
59 in both dosages in controlling crack widths, specifically in the serviceability range. Although the
60 overall response in terms of load-deflection behaviour was comparable for all specimens, smaller
61 deflections and higher load bearing capacities were obtained for specimens with fibres. Døssland
62 [20] carried out three-point bending test under a concentrated load on R/FRC slabs of 3600×1200
63 mm. The R/FRC slabs containing 0.7% of fibres and a reinforcement ratio as low as $\rho_s = 0.07\%$
64 showed less deflection compared to the control specimen without fibres and having a $\rho_s = 0.33\%$.
65 However, at a deflection of 20 mm a softening behaviour was observed for the R/FRC slabs.
66 Despite the advantages of application of steel fibres in reinforced concrete tension ties and statically
67 determined structural elements under uniaxial bending, the highest advantages of this material
68 would be in statically redundant structures in which stress redistribution may occur [21]. The
69 greater number of yield lines needed for the formation of a failure mechanism, the higher would be
70 the contribution of the fibres in the load carrying capacity of the structure [22]. Facconi et al. [23]
71 tested a thin slab of 4200×2500×80 mm which was once reinforced with 91 kg/m³ of rebars and
72 once with an optimized combination of 43 kg/m³ of rebars and 25 kg/m³ of steel fibres (in total 68
73 kg/m³). There was an opening in the slab and it was continuously supported on all sides. While the
74 R/C slab suffered from a sudden decay of stiffness after cracking, the R/FRC slab maintained its
75 stiffness up to a much higher load and at collapse, smaller crack widths and higher maximum load

76 were achieved for this specimen. Fall et al. [24] tested octagonal slabs with the reinforcement ratio
77 being different in the two directions to create a weaker side in the slabs. The addition of 35 kg/m^3 of
78 steel fibres reduced the deflection of the slabs under loading and the presence of fibres led to a more
79 uniform load transfer at the position of the supports through a smearing effect.

80 The importance of structural indeterminacy in fibre reinforced structures is reflected in the *fib*
81 Model Code 2010 (MC 2010) [25] where the use of fibres as sole reinforcement is permitted only if
82 a certain level of ductility is provided to structural elements. In this regard two-way slabs are of
83 particular interest as they may allow a significant stress redistribution when properly reinforced.
84 This may explain why steel fibres have been extensively adopted in construction of flat slabs, slabs
85 on pile, and slab on ground. Higher flexural strength and much higher ductility has been reported
86 for FRC slabs on grade as compared to similar concrete slabs made of plain concrete [26]–[28].
87 Slabs on pile and elevated slabs have been successfully built and tested with only steel fibres with a
88 dosage in the range of 45 kg/m^3 and 100 kg/m^3 [29], [30] for industrial, commercial, and residential
89 buildings, with the presence of continuous steel rebars for connecting columns. To check the
90 structural behaviour of SFRC slabs without any longitudinal reinforcement, an elevated flat slab
91 with 9 bays built on 16 circular columns with a 6 m span for each panel and a thickness of 200 mm,
92 reinforced only with 70 kg/m^3 of steel fibres (60 mm long and with a diameter of 1 mm) was tested
93 in Limelette (Belgium) both in SLS and ULS conditions [31], [32]. A fully plastic behaviour was
94 observed at the maximum load which occurred at a load higher than the prediction. However, the
95 results raised some doubts about the overall ductility of the structure.

96 Despite all efforts devoted to better understand the structural behaviour of SFRC members, there is
97 still a lack of experimental evidence on the behaviour of this material in statically redundant
98 structural configurations. Therefore, a wide experimental programme is designed to investigate
99 some issues regarding the structural benefits and limitations of SFRC. In this paper, six concrete
100 slabs supported at the middle of each side are tested under a biaxial bending condition. Two of the
101 specimens are only reinforced with 35 kg/m^3 of steel fibres, two are reinforced with 35 kg/m^3 of

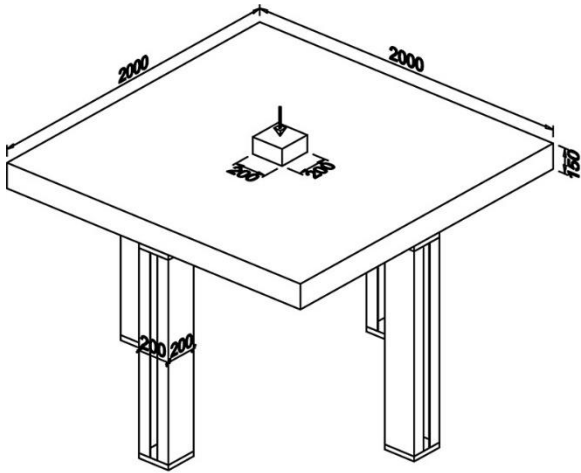
102 reinforcing bars in each direction, and two are reinforced with the combination of both the two
103 reinforcing solutions. Specifically, this work is aimed at investigating:

- 104 - the effectiveness of steel fibres versus reinforcing bars in terms of load bearing capacity;
- 105 - the ductility of SFRC slabs, particularly with reference to that required to activate the
106 resistant mechanisms usually considered for R/C bi-dimensional elements according to
107 limit analysis;
- 108 - at what extent the limited ductility of SFRC material in biaxial bending (assumed at least
109 $\varepsilon_{Fu}=2\%$ in the Model Code) may affect the overall structural response of a R/FRC
110 element, in order to verify, as occurs in uniaxial bending, if it can reduce the ductility
111 guaranteed by conventional reinforcement.

112 To achieve these aims, measurements were carried out on the deflection and cracking behaviour of
113 the plates and comparisons were made based on test results. Furthermore, a yield line approach was
114 adopted to estimate the ultimate bearing capacity and the results are compared with the
115 experimental maximum loads.

116 **2. EXPERIMENTAL PROGRAMME**

117 The experimental programme reported herein is part of a more extensive experimental campaign
118 activated during the construction of the first industrial building in Italy, characterized by three
119 different SFRC slab types: a foundation slab on piles (1436 m²), two elevated solid slabs in R/FRC
120 (540 m²) and a partially prefabricated R/FRC slab supported on P/FRC beams (1171 m²) [33].
121 Together with the six 2000×2000×150 mm concrete slabs reinforced with steel fibres and/or steel
122 reinforcing bars tested under a central point load, six cubes and fourteen standard notched
123 specimens were tested respectively in uniaxial compression and in a three-point bending setup
124 (according to EN 14651 [34]) for material characterization. The test setup and a general scheme of
125 the slab specimen is shown in Fig. 1.



(a)



(b)

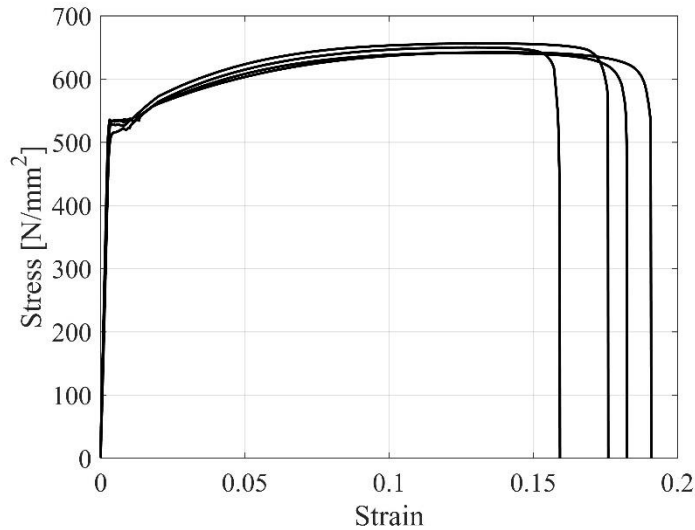
126
127 *Fig. 1- (a) Sketch of the experimental setup; (b) an image of a loaded slab.*

128 **2.1 Materials and specimen preparation**

129 *Materials*

130 The concrete used in the present investigation is self-compacting with a mean compressive strength
 131 of 58 MPa determined on six cubes with a side of 150 mm. Its composition consists of 380 kg/m³ of
 132 CEM IV 42.5R and 100 kg/m³ of calcium carbonate filler. The water/binder ratio is 0.36 and 1.2%
 133 by weight of cement of superplasticizer is added. The mixture contains 0/4 sand, 0/8 sand and 8/14
 134 gravel in dosages of 450 kg/m³, 850 kg/m³, and 425 kg/m³ respectively. The same mixture was used
 135 to produce the plain concrete and the SFRC mixtures, in which 35 kg/m³ of double hooked-end
 136 steel fibres were added. The steel fibres used were 60 mm long with a diameter of 0.9 mm.
 137 According to the manufacturer, the tensile strength is 1500 MPa and the Young's modulus is 210
 138 GPa.

139 The properties of the rebar steel were assessed on four specimens. The average yield and ultimate
 140 strengths of the reinforcing steel were found to be 527 MPa and 647 MPa, respectively. The average
 141 ultimate strain obtained from the four specimens was 18.75%. Fig. 2 shows the nominal stress-
 142 strain curves obtained for the specimens.



143

144 *Fig. 2- Uniaxial tension test on rebars.*

145 *Specimen preparation*

146 As anticipated in the introduction, two slabs were reinforced only with steel fibres (SFRC1,
 147 SFRC2), two were cast with plain concrete and reinforced with 35 kg/m^3 of rebars in each direction
 148 ($12 \Phi 12$ mm rebars equally spaced in both directions) (R/C1, R/C2), and in the last two ones steel
 149 fibres and rebars were combined (R/FRC1, R/FRC2). In the R/C specimens the reinforcing rebars
 150 were placed at the bottom with a minimum cover of 30 mm from each side. During casting, the
 151 concrete was pumped from a truck mixer to the centre of the formworks to allow a radial flow of
 152 the fresh concrete and no vibration was carried out. It has been shown that fibres tend to align
 153 perpendicularly to the flow direction in concrete slabs [35]–[38] which increases the fibre
 154 effectiveness [39]. After casting, all specimens were covered with wet burlaps and kept moist for a
 155 couple of days. Then, they were kept in atmospheric condition until the day of testing. The
 156 $600 \times 150 \times 150$ mm prismatic beams were cast together with the slabs and were notched at the mid-
 157 span to a depth of 25 mm. The six cubes were tested at 35 days in the conditioning room in the lab
 158 at 20°C and RH 90%.

159

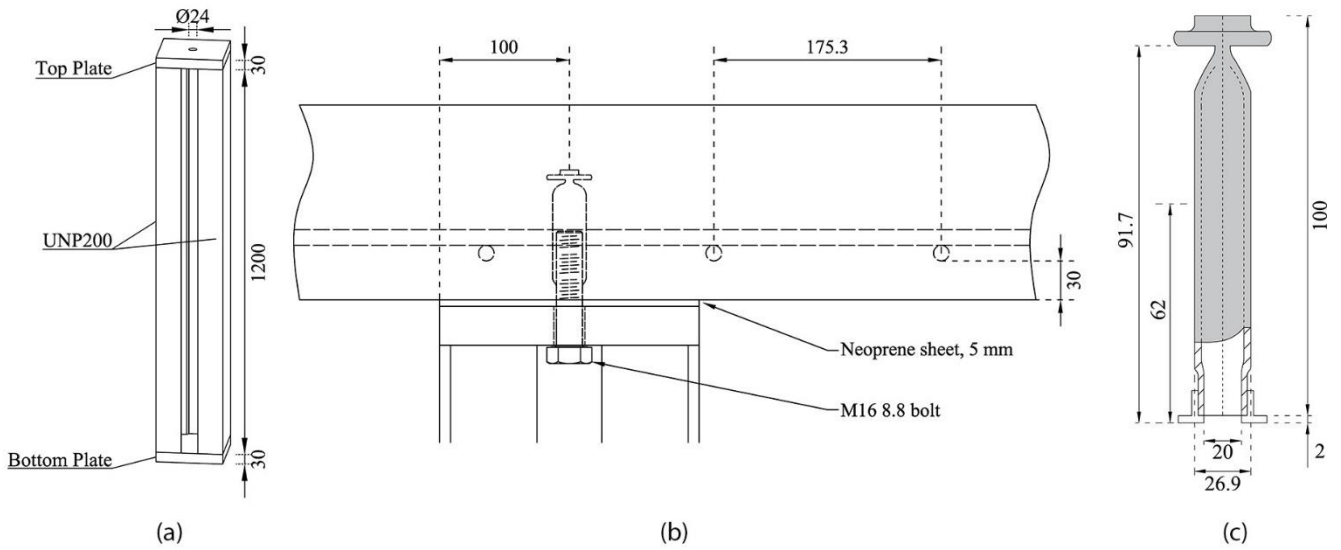
160 **2.2. Bending test on notched beams**

161 The tests were carried out controlling the Crack Mouth Opening Displacement (CMOD) that was
162 measured by a clip gauge introduced between two aluminium supports glued at the tip of the notch.
163 According to the MC 2010, characterization of the post-peak residual strength of FRC in a three-
164 point bending test is achieved by considering the residual flexural tensile strength, $f_{R,i}$ $i=1:4$, at
165 $CMOD_i= 0.5, 1.5, 2.5,$ and 3.5 mm. From the fourteen specimens, 5 were tested at 34 days of age, 5
166 were tested with the first SFRC slab test at 167 days, and 4 specimens were tested at the end of the
167 complete experimental campaign at 220 days.

168 **2.3. Slab tests**

169 *Loading and support conditions*

170 The load was applied in the centre of the specimens by means of an electro-mechanical jack with a
171 maximum capacity of 1000 kN by adopting a displacement control procedure. A constant
172 displacement rate equal to $20 \mu\text{m}/\text{sec}$ was imposed to the steel loading head characterized by a cross
173 section of 200×200 mm. A neoprene sheet of $220 \times 220 \times 30$ mm was placed under the loading point.
174 The slabs were supported at the middle of each side. The supports consist of two UNP 200 profiles
175 that were placed 50 mm apart and were welded on a top and bottom steel plate with dimensions of
176 $200 \times 200 \times 30$ mm. A 5 mm thick neoprene sheet was placed between the specimen and the support.
177 There was a hole on the support top plate to facilitate the insertion of a M16 bolt that was screwed
178 in a threaded fixing anchor device embedded in the specimens to create a bilateral support. The
179 length of the anchorage bush was 100 mm, with a threaded length of 62 mm, while the threaded
180 length of the bolt was 50 mm. Figure 3 shows the details of the support and the reinforcement
181 detailing.

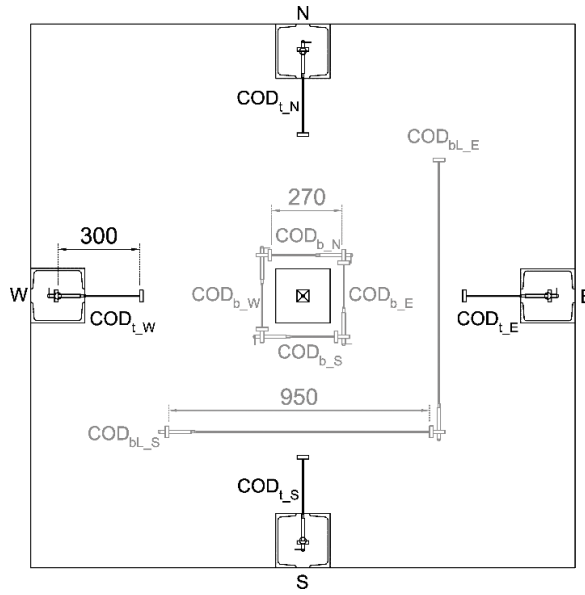


182

183 *Fig. 3- Details of the support: (a) dimensions of the steel support; (b) details of the anchorage and*
 184 *reinforcement spacing; (c) drawing of the anchorage device.*

185 *Instrumentation*

186 A total of 11 displacement transducers were used for each test: 1 for the slab deflection, measuring
 187 the vertical displacement from the bottom at the centre of the slab and 10 to detect crack openings.
 188 The location of the 10 gauges aimed at measuring crack openings is indicated (Fig. 4). For coding
 189 the instruments, COD (crack opening displacement) is followed first, by a subscript “t” if the
 190 instrument is placed on top of the slab or “b” if placed at the bottom of the slab, and then followed
 191 by a letter “L” for the two instruments with a longer gauge length. The last subscript shows the
 192 position of the instrument in the plane of the specimen with N standing for North, and W, S, and E
 193 standing for the other cardinal points. The nominal gauge length of each instrument is also given in
 194 Fig. 4. The instruments on top face of the slab were placed over the supports to capture possible
 195 negative cracking, and at the bottom of the slab four transducers were placed at 150 mm from the
 196 centre in a squared configuration and those with a longer gauge length were placed at 500 mm from
 197 the centre. To measure the vertical deflection and the crack openings by instruments COD_{bL-S} and
 198 COD_{bL-E}, potentiometer transducers were used, and the rest of the measurements were carried out
 199 by Linear Variable Deformation Transducers (LVDT).



200

201 *Fig. 4 - Code and position of the ten instruments measuring crack opening: four at the top (black)*
 202 *and six at the bottom (grey).*

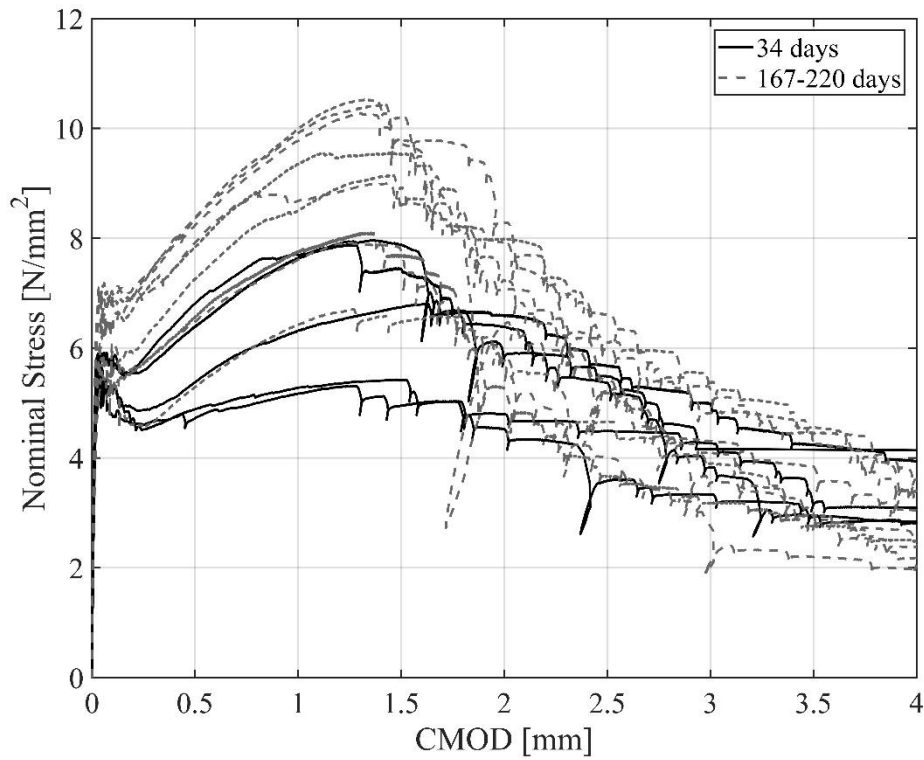
203 3. EXPERIMENTAL RESULTS

204 3.1 Bending tests on notched beams

205 The nominal stress-CMOD curves for all fourteen specimens tested at different ages are shown in
 206 Fig. 5 and the statistical parameters obtained for flexural tensile strength, $f_{ct,fl}$, and post-peak
 207 residual strength values, $f_{R,1}$, $f_{R,2}$, $f_{R,3}$, and $f_{R,4}$ are reported in Table 1. The results are treated
 208 separately for specimens tested at 34 days and those tested at an older age. It is evident that there is
 209 a shift in material properties going from 34 days to 167 and 220 days. While classifying the SFRC
 210 according to provisions of MC 2010 at 34 days leads to a “3c” material, taking into account the
 211 specimens tested at 167 and 220 days, a “5b” material is obtained. The use of a CEM IV cement
 212 may be a reason for the considerable strength increase with the curing time [40]. It is interesting to
 213 observe that even if the first cracking strength ($f_{ct,fl}$) increases for only 11%, the residual strength
 214 values of $f_{R,1}$ and $f_{R,2}$ (mainly related to SLS) experience a 30% increase of the average value. In
 215 case of larger CMOD values, less significant effects are observed: a 6% increase of $f_{R,3}$ average
 216 value and a slight decrease of 2.3% for $f_{R,4}$. Clearly, for the specimens tested in this study, age of the

217 specimens has the most significant effect on strength values in the range of CMOD that corresponds
218 to the SLS. Comparable observations were reported by Buttignol et al. in [41], where SFRC
219 specimens 1 year and 10 years aged were tested in a four-point bending test. The results reported by
220 the authors showed that there was a considerable increase in the peak and post-peak residual
221 stresses up to a CMOD of 1 mm, while in the softening branch only a marginal strength increase
222 was observed. In the present work, the coefficient of variation (CV) for $f_{R,1}$ and $f_{R,2}$ reduced with age
223 while, for other strength values reported, the CV increased or did not change over time.
224 Nevertheless, the CV falls approximately in the range of 15% to 20% for all the residual strength
225 parameters and for both the groups.

226 In the MC 2010 two limitation are proposed for SFRC to be considered as a structural material,
227 which are $f_{R1,k}/f_{ctk,fl} > 0.4$, and $f_{R3,k}/f_{R1,k} > 0.5$ to limit the brittleness in uniaxial tension behaviour
228 guaranteeing a minimum toughness in bending. Considering the results obtained here, over time the
229 ratio of $f_{R,1k}/f_{ctk,fl}$ increased from 0.72 to 1 and the ratio $f_{R,3k} / f_{R,1k}$ reduced from 0.81 to 0.65. The
230 latter indicates that over time, the same material tends to exhibit a less ductile behaviour in the post-
231 peak range.



232

233 Fig. 5 - Stress-CMOD results obtained from the bending tests.

234 Table 1- Statistical parameters of the strength values obtained from the three-point bending test
 235 divided into two categories based on the testing age, in [MPa].

Group of specimens		$f_{ct,fl}$	$f_{R,1}$	$f_{R,2}$	$f_{R,3}$	$f_{R,4}$
34 (5 specimens)	mean	5.7	5.64	6.49	4.92	3.48
	Std*	0.21	0.92	1.27	0.87	0.65
	CV**	0.04	0.16	0.2	0.18	0.19
	Charac-Normal ***	5.21	3.48	3.54	2.88	1.96
	Charac-LogN****	5.22	3.82	3.99	3.1	2.24
167+220 (9 specimens)	mean	6.32	7.36	8.73	5.2	3.39
	std	0.53	1.05	1.22	0.96	0.88
	CV	0.08	0.14	0.14	0.18	0.26
	Charac-Normal	5.28	5.3	6.34	3.32	1.67
	Charac-LogN	5.34	5.39	6.48	3.5	1.97

236 *Standard deviation

237 **Coefficient of Variation

238 ***Characteristic value considering a normal distribution

239 ****Characteristic value considering a log-normal distribution

240 3.2 Slab test results

241 *Load-deflection behaviour*

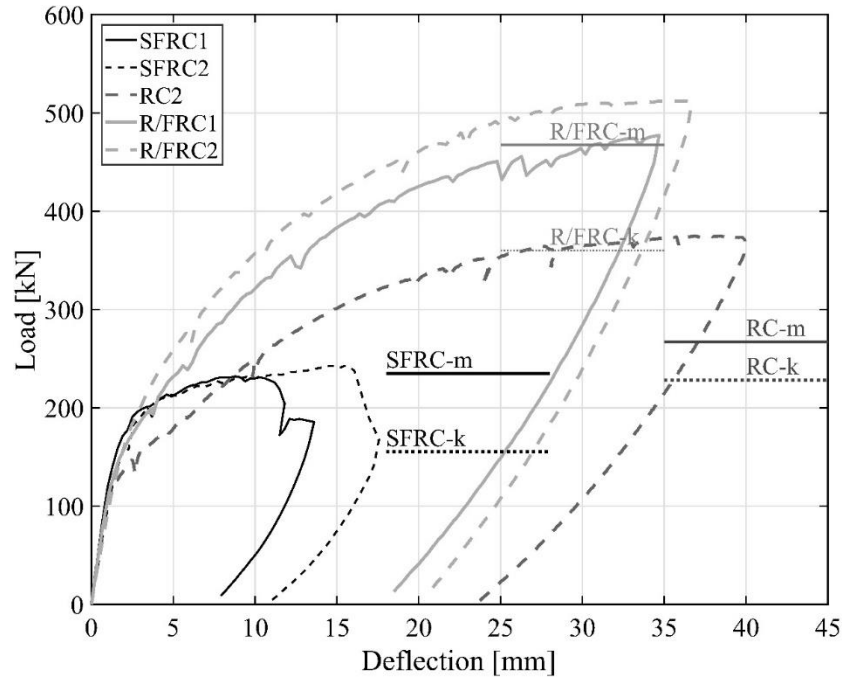
242 The results obtained from the load-deflection behaviour of the slabs are shown in Fig. 6. Due to
243 problems with recording the deflection data of RC1 specimen, the results of this test are not
244 reported in this figure.

245 A quick glance at the deflection curve of the specimens reveals the substantial effect of steel fibres
246 on the overall structural response of the elements. A major contribution of fibres is evident at
247 approximately 120 kN, where R/C slabs undergo a sudden loss of stiffness. The stiffening effect
248 brought by the steel fibres in the R/FRC slabs, leads to a stark difference between the deflection
249 behaviour of the R/C and R/FRC slabs. After 200 kN, the deflection of the R/FRC slabs is less than
250 half of the deflection of the R/C specimens. Even the slabs that are reinforced only with steel fibres
251 show less deflection in this range of loading in comparison to the R/C slabs. It is worth noticing the
252 very different deflection response of the R/C and R/FRC slabs reported in this study, and those
253 reported in [19] where a four-point bending test was chosen to compare the behaviour of R/C and
254 R/FRC slabs. Unlike the results presented here, the deflection of the R/FRC slabs, tested by Pujadas
255 et al. was only slightly smaller than the R/C ones in the SLS range. This may be a clear indication
256 of the superior efficiency of the application of fibres in redundant structural schemes, where higher
257 stress redistribution coupled with multiple cracking may occur.

258 The structural response of the SFRC specimens is characterized virtually by a bilinear behaviour. A
259 first branch that goes up to around 190 kN for both of the specimens, and then a hardening
260 behaviour controlled by the pull-out mechanism of the fibres. A 5% and 10% increase in the load
261 level is observed for the SFRC1 and SFRC2 slabs during the hardening behaviour, before softening
262 phase associated to crack localization occurs. The maximum load attained by the SFRC specimens
263 is 232 kN and 243 kN at a deflection of 10.6 mm and 15.5 mm respectively for the SFRC1 and
264 SFRC2 elements. Afterwards, a softening branch is observed and at a deflection of 13.5 mm for
265 SFRC1 and 17.4 mm for SFRC2 the tests were stopped.

266 Steel fibres also largely affect the ultimate load bearing capacity of slab elements for elevated
267 deflections if combined with conventional reinforcement. At a deflection of 35 mm the R/C

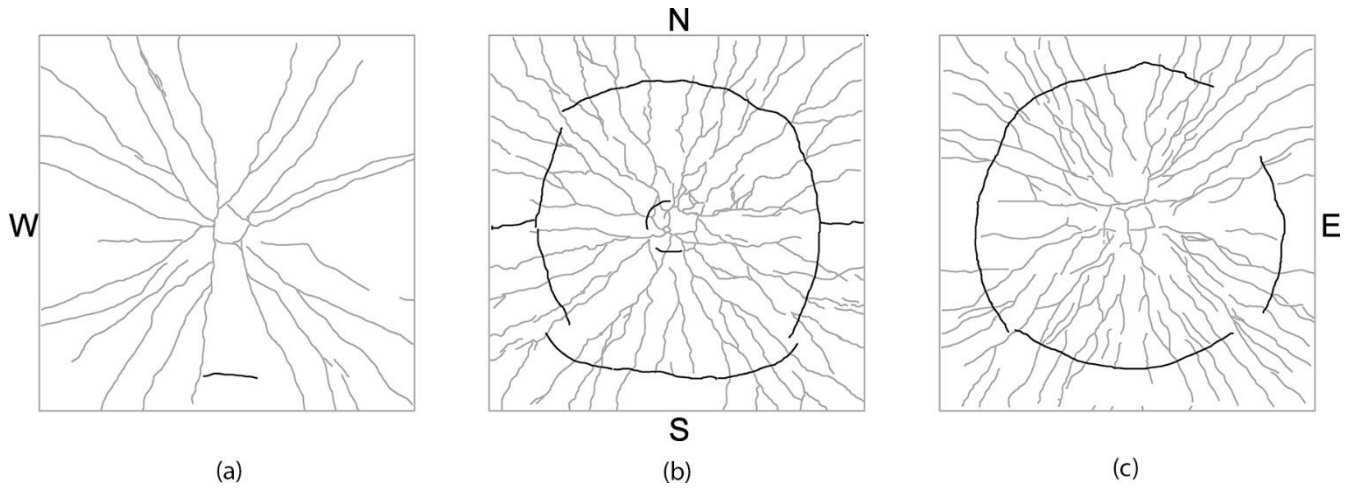
268 specimens carry an average load of 365 kN, while the R/FRC companions sustain an average load
 269 of 494 kN which is 35% higher. The presence of fibres in the R/FRC specimens is responsible for
 270 an almost 130 kN of load difference between the R/C and R/FRC slabs.



271
 272 *Fig. 6 - Load-deflection results for the slabs tested and the ultimate load bearing capacity*
 273 *prediction obtained from yield line analysis based on average and characteristic material*
 274 *properties.*

275 *Crack Patterns*

276 The final crack patterns for SFRC2, RC2, and R/FRC2 slabs are shown in Fig. 7. The cracks which
 277 appeared on the top of the slab elements are drawn with black lines, while the bottom cracks are
 278 marked with grey lines. The crack patterns show that there is a considerable difference in the extent
 279 of cracking between the SFRC slabs and those reinforced with rebars. Furthermore, the evolution of
 280 a circular crack on the top face of the R/C and R/FRC specimens is visible, which is a common
 281 mechanism for slab members under concentrated loading [42] if a boundary restraint is introduced.
 282 SFRC slabs are not capable to reach the level of ductility required to activate the kinematic
 283 mechanism of failure that comprises the cracking of the top surface of the slabs.



284 (a) (b) (c)

285 *Fig. 7 - Final crack patterns for (a) SFRC2 (b) RC2, and (c) R/FRC2 slabs. Bottom cracks are*
 286 *shown in grey and top cracks in black.*

287 *Bottom cracking*

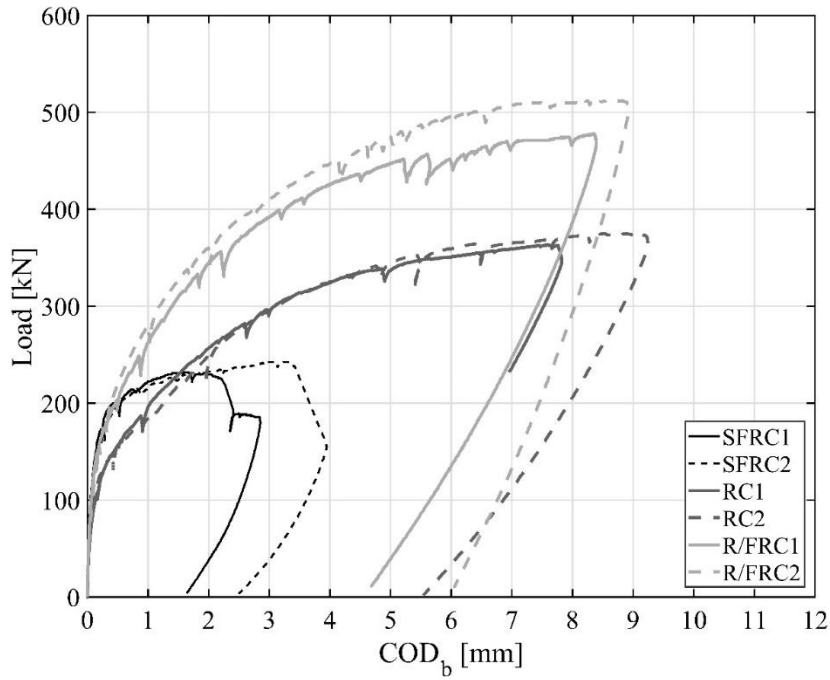
288 The results obtained from the instruments installed at the bottom of the specimens to capture the
 289 cracking behaviour, are shown in Fig. 8 and Fig. 9. Fig. 8 illustrates the load-COD_b measurements
 290 and Fig. 9 concerns the COD_{bL} measurements. Due to technical problems the load-COD_{bL} curve for
 291 the RC1 specimen starts at a load of around 150 kN, which is marked by a circle on the figure. The
 292 COD values reported in Fig. 8 and Fig. 9(a) are the average values of the corresponding
 293 instruments. However, in order to examine the cracking behaviour of each slab in the two
 294 directions, Fig. 9(b) exhibits the load-COD_{bL} measurements carried out for specimens SFRC2, RC2,
 295 and R/FRC2 separately for both COD_{bL-S} and COD_{bL-E}.

296 Inspecting the bottom cracking behaviour of the slabs and zooming into the curves obtained, it can
 297 be noticed that the load-COD curves for RC1 and RC2 specimens diverge from those of the SFRC
 298 and R/FRC series at an earlier stage, as compared to the deflection response. The overall structural
 299 response of the slabs is less sensitive to the very local propagation of cracks. However, similar to
 300 the deflection behaviour, in the proximity of 120 kN, both COD_b and COD_{bL} measurements show a
 301 noticeable increase in the crack opening values. Looking at COD_{bL-S} and COD_{bL-E} measurements
 302 separately for SFRC2, RC2 and R/FRC2 slabs shown in Fig. 9b, it is observed that in each

303 specimen the COD recorded by one of the instruments grows faster compared to the other one. In
304 the results displayed for the three specimens, the crack opening measured by COD_{bL-E} registers
305 larger crack openings compared to COD_{bL-S} .

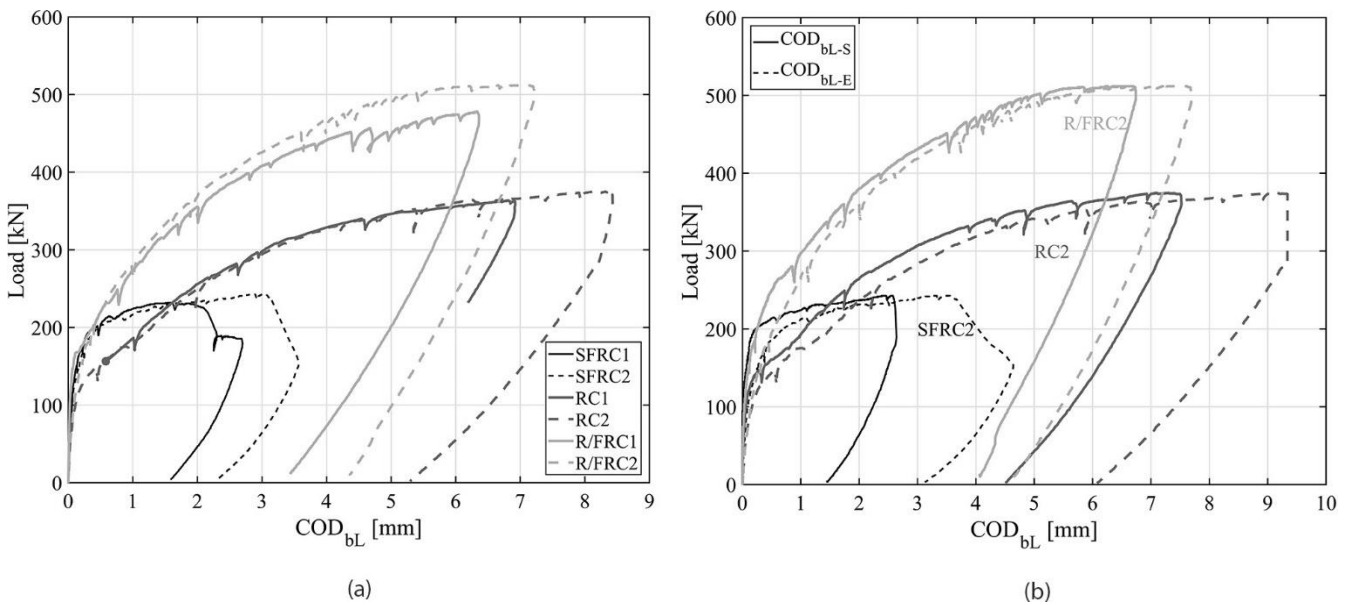
306 After 120 kN, in the SLS range, the effect of steel fibres in controlling the crack opening is easily
307 recognized even without rebars. In the SFRC specimens the presence of steel fibres alone, leads to
308 COD values that are half to one-third of the COD values measured in the R/C slabs and this
309 observation holds until the point that the SFRC specimens go through an almost plastic
310 deformation. The same comparison holds between the R/FRC and R/C elements.

311 For the SFRC slabs, although the two specimens are nominally identical, the COD values registered
312 on COD_b and COD_{bL} measurements at the onset of the softening phase are different while
313 comparable peak loads are obtained for these specimens. It is indeed pointed out that Fig. 8 and Fig.
314 9(a) are based on the average values of the measured CODs and they do not represent the
315 measurement of a single instrument. Considering the recordings of each single COD_b measurement,
316 it could be seen that for SFRC1 at maximum load, the reading of the four instruments vary between
317 1.45 and 2.55 mm and, soon after the softening behaviour, the instruments that pass over the
318 localized crack start to register larger values, while other instruments register small variation in the
319 COD. At the end of the test the COD_b measurements fall in the range of 1.66 to 4.22 mm for the
320 SFRC1 slab. Comparable results are obtained for the SFRC2 slab. This is better shown in the Fig.
321 9(b) where for the SFRC2 specimen, as the softening phase unfolds, the COD_{bL-E} records increasing
322 COD values associated to the localized crack, while the opening of the crack measured on COD_{bL-S}
323 remains constant.



324

325 Fig. 8- The average Load- COD_b results measured by COD_{b-N} , COD_{b-W} , COD_{b-S} , and COD_{b-E}
 326 instruments.



327

328 Fig. 9 - SFRC2, RC2, and R/FRC2 specimens: (a) average Load- COD_{bL} results measured by
 329 COD_{bL-N} , COD_{bL-W} , COD_{bL-S} , and COD_{bL-E} instrument; (b) individual Load- COD_{bL} results
 330 measured by COD_{bL-S} and COD_{bL-E} instruments.

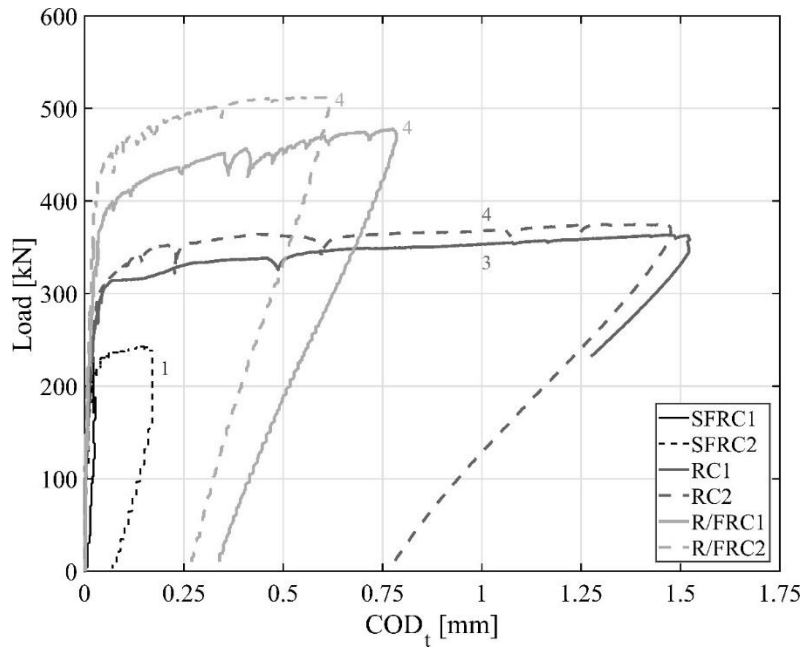
331 The significance of limiting crack widths to enhance durability of concrete structures cannot be
332 overrated. There seems to be a crack width threshold below which the permeability of concrete is
333 not affected. While according to Otieno et al. [43] this threshold depends on concrete mixture and
334 properties, other studies mention a crack width approximately between 0.05 and 0.1 mm as the
335 threshold [6,44,45]. At 0.05 mm of COD_b , the load carried by the SFRC and R/FRC slabs are 35%
336 and 25% more the load carried by the R/C slabs, and at 0.1 mm the difference is increased to almost
337 40% and 30%. The CODs reported are measured along the length of the instrument gauge and
338 indicate the cumulative COD along the gauge. Therefore, there are chances that for the R/C and
339 R/FRC slabs higher number of cracks with a narrower width would be recorded when compared to
340 the SFRC slabs. Furthermore, the increased tortuosity of the crack surfaces in FRC mixtures may
341 play a role in further reduction of cracked concrete permeability [46].

342 *Top cracking*

343 The results related to the cracking at the top surface of the slabs which are recorded at the position
344 of the supports are presented in Fig. 10. The COD_t values are averaged between the number of
345 instruments that have actually registered the propagation of a crack. The number shown on each
346 curve gives the number of instruments that have passed over a crack.

347 According to these results it is evident that negative cracks develop only at late stages of loading.
348 As mentioned earlier, the SFRC specimens do not experience negative cracking except for a short
349 crack that propagates at the position of COD_{t-s} for SFRC2 slab. This crack opens up at 213 kN and
350 reaches a COD of 0.17 mm at the end of the test. However, in case of specimens reinforced with
351 rebars a complete circular negative crack pattern was developed.

352 The negative cracking for the R/C slabs starts to propagate at about 310 kN of load; for the R/FRC1
353 and R/FRC2 specimens the initiation of the negative cracks is respectively at 400 and 450 kN.
354 Before stopping the test, the average COD_t measured for the R/C specimens are considerably larger
355 than those measured for the R/FRC slabs. The effectiveness of steel fibres in controlling the
356 opening of the negative moment cracks in the absence of top reinforcement is easily appreciated.



357

358 *Fig. 10 - Average Load-COD_t results measured by COD_{t-N}, COD_{t-W}, COD_{t-S}, and COD_{t-E}*
 359 *instruments. The number on each curve shows the number of instruments that have actually*
 360 *recorded the propagation of a crack.*

361 **4. DISCUSSION OF RESULTS**

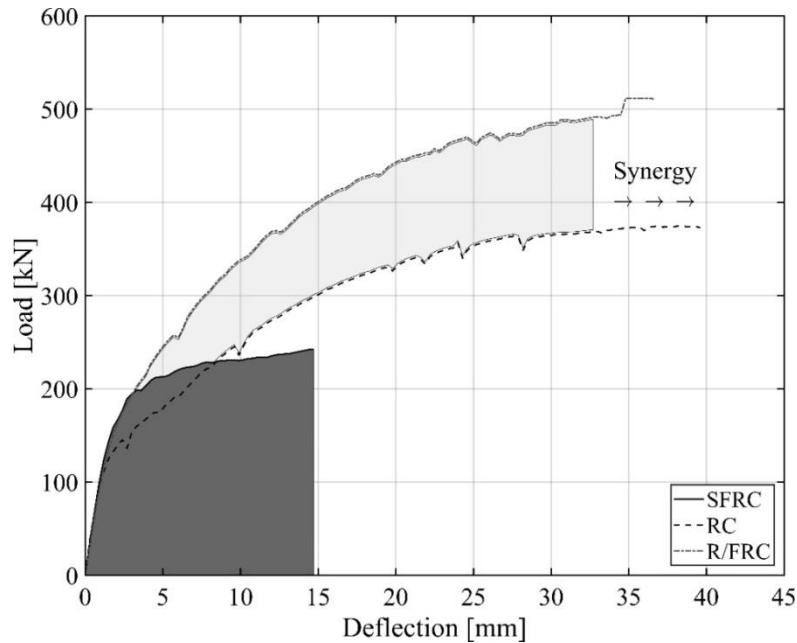
362 Comparing the SFRC and R/C solutions in which 35 kg/m³ and 70 kg/m³ of steel is available
 363 respectively, it is evident that twice the amount of steel weight in the R/C slabs with respect to the
 364 SFRC specimens, accounts for only a 55% increase in the load bearing capacity. It should also be
 365 noticed that the two layers of reinforcing steel are positioned exactly in the tensile region of the
 366 slabs, while the steel fibres are dispersed in the whole volume of the elements. Seemingly, the 3D
 367 spatial distribution of steel fibres leads to a more efficient stress distribution and consequently, a
 368 larger load bearing capacity when juxtaposed with the R/C companions. An interesting comparison
 369 could be also obtained by imagining to half the reinforcement introduced in the R/C structure, in
 370 order to have a conventional reference at the same amount of steel: in this case a similar cracking
 371 load and a similar ductility could be obtained, but with an ultimate bearing capacity of about 185
 372 kN, that corresponds to a loss of about 23% of bearing capacity for the same amount of steel when
 373 compared to the SFRC solution.

374 Despite the efficiency in load carrying capacity, the shortcoming of the SFRC specimens is the
375 lower ductility. At 10 and 15 mm of deflection, the SFRC slabs go through a softening phase, while
376 the R/C ones continue on a plateau even at 40 mm of deflection. The limited ductility affects also
377 the maximum load that is carried by the SFRC slabs. At a COD_b between 2 to 3 mm the softening
378 phase is reached in these specimens, which prevents the activation of negative cracks thus also
379 limiting the maximum load bearing capacity of the SFRC solution.

380 In the R/FRC slabs, the presence of rebars allow steel fibres to stay effective for a higher range of
381 deformation. In the R/FRC slabs at COD_b values of more than 8 mm the effect of fibres is still
382 present, and no major load reduction is observed. Hence, in the R/FRC slabs, not only the high
383 ductility is assured, but the range of deflection in which the fibres are effective is increased. The
384 effectiveness of fibres wears off at a certain crack opening when reached on a single crack. The
385 diffused cracking due to presence of rebars, limits the COD on each single crack which in turn
386 keeps the fibres active for larger deflection. Nevertheless, it is noticed that in terms of load carrying
387 capacity, the interaction of steel fibres and rebars can not be fully uncoupled and the addition of the
388 SFRC and R/C curves in the load direction does not yield the R/FRC curves.

389 The positive interaction between steel fibres and reinforcing rebars may be explained also
390 considering the area below the load deflection curves. In Fig. 11, the dark grey is the area under the
391 load-deflection curve for the average behaviour of the SFRC elements and the light grey depicts the
392 same area, however filling the area between the load-deflection response of the R/FRC and R/C
393 slabs, namely, the effect of fibres in R/FRC slabs: by computing the energy values as shown in Fig.
394 11, the light grey area is around 2.1 kNm, while the dark grey area is 3.1 kNm. The presence of
395 steel fibres in the R/FRC slabs is responsible for providing more energy compared to the effect of
396 fibres in the SFRC slabs. While the topic of synergy between different types of fibres has been
397 extensively studied [47-50], there seems to be also a synergetic effect in the fibre/rebar interaction.
398 While in the present study the R/C and R/FRC specimens were unloaded just to avoid any possible
399 damage to the instruments, it could be considered that the R/C and R/FRC slabs could have

400 undergone higher levels of deflection, in which case the synergy effect could have been better
 401 computed. It is worth to note that the negative bending moment activated along the top crack in the
 402 R/FRC slabs contributes to this effect.



403

404 Fig. 11- Fibre/rebar synergic effect.

405 **5. ULTIMATE LOAD PREDICTION**

406 A yield line approach is adopted to predict the ultimate load bearing capacity of the slab elements.
 407 Application of yield line method to fibre reinforced concrete slabs is a common practice which has
 408 been adopted elsewhere with satisfactory predictions of the ultimate load [51]–[53]. A yield line
 409 analysis considers an ultimate plastic behaviour for the material which is not the case for a SFRC
 410 showing a softening behaviour. However, an almost plastic behaviour in the moment-curvature
 411 response allows for the implementation of this method to a softening material like the one
 412 investigated. The minimum ultimate load obtained according to a yield line configuration
 413 corresponds to a circular failure mechanism which agrees with the experimental crack pattern. The
 414 yield line pattern is shown in Fig. 12 and the ultimate load based on this failure mechanism is

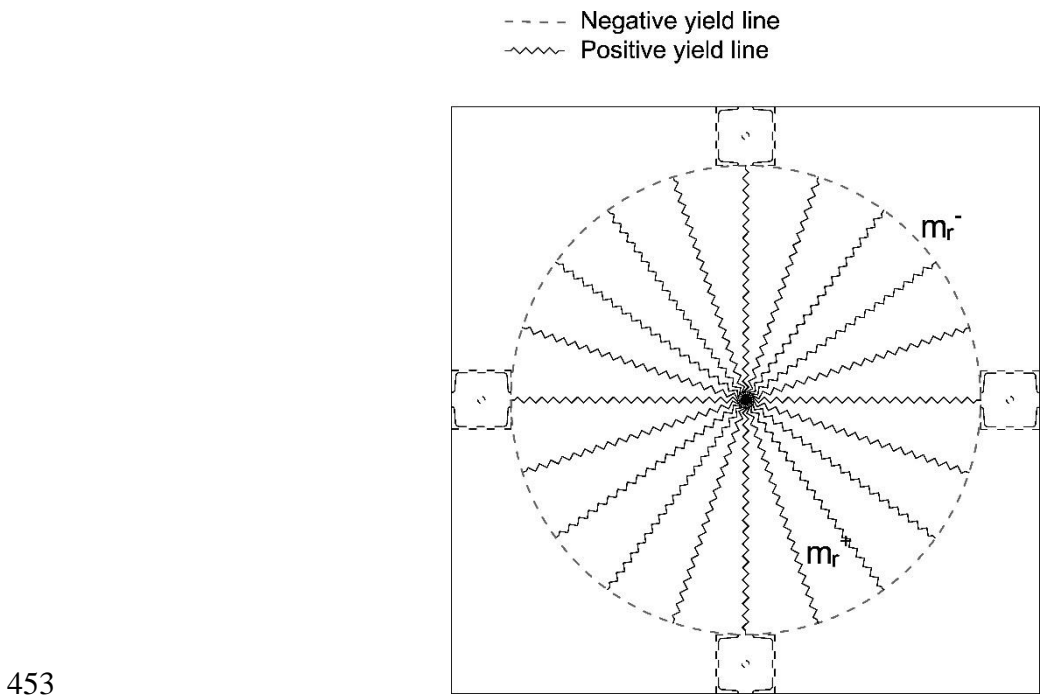
415
$$P_u = 2\pi(m^+ + m^-)$$

416 (1) where m^+ and m^- are respectively positive and negative ultimate resistant bending moment. The

417 computations are carried out once based on the mean values of material properties and once with
418 the characteristic values both for steel and concrete. For the SFRC solution the material properties
419 obtained from the tests carried out on 167 and 220 days are used, and a linear-elastic / linear-
420 softening behaviour is adopted for the behaviour of fibre concrete in tension. To compute the
421 sectional resisting bending moment a characteristic length equal to the thickness of the elements is
422 chosen. No sedimentation effects were taken into account and therefore for SFRC slabs a symmetric
423 isotropic resistant bending moment is computed ($m^+ = m^-$). For the reinforcing bars, a plastic
424 behaviour without hardening is first considered. The results obtained from the analysis for each slab
425 type and for both cases, by assuming both the mean and the nominal characteristic material
426 properties, are shown by a line segment in Fig. 6 and are respectively specified by a “m” and “k”
427 letters.. The predicted ultimate bearing capacity of the SFRC specimens using the mean values of
428 material properties, almost exactly catches the ultimate experimental load, however, for the R/C
429 slabs, given that the hardening of the reinforcement is not introduced in the model, safe predictions
430 are made for the maximum load. If the ultimate strength was taken into account, the ultimate load
431 would increase of about 26%, growing from 268 kN to 314 kN.

432 Due to the specific boundary conditions chosen in the present study, negative moment cracks were
433 not formed for the SFRC specimens; however, the ultimate limit state failure mechanism assumed,
434 comprises also cracks on the top surface of the slabs. Hence, while the ultimate load prediction for
435 the SFRC slabs based on the complete circular fan gives a close prediction of the experimental
436 maximum loads, the lack of the negative resisting moment in the formulation could have led to a
437 more conservative prediction. This difference could be due to the lower CMOD in the slab test at
438 the peak than the 2.5 mm considered in the calculations. In fact the cumulative average COD_{bL} at
439 the peak measured around 2-3 mm over more than 8 cracks, without any localization. Therefore, the
440 actual stresses at the position of the cracks are closer to $f_{R,1}$ and $f_{R,2}$ values rather than the $f_{R,3}$ value
441 which is introduced in the computations.

442 The fact that no negative cracks appeared in the SFRC slabs deserves more attention. Despite the
 443 lack of the negative cracking on the specimens, the introduction of the negative resisting moment in
 444 the ultimate load prediction gave satisfactory results for the present example, but it cannot be
 445 guaranteed as a rule. Therefore, the application of yield lines kinematic approach according to limit
 446 analysis to compute the ultimate bearing capacity of FRC elevated slabs which may not show
 447 enough ductility to activate the complete failure mechanism may sacrifice safety of the overall
 448 structural behaviour. In this respect, provision of a minimum level of conventional reinforcing steel
 449 may well provide the required ductility. Finally, the average values in case of R/FRC slabs taking
 450 into account in the computation of the rebars contribution the steel yielding strength, is very close to
 451 the experimental load, thus showing that fibre contribution acting on both positive bending cracks
 452 was reduced.



453
 454 Fig. 12 - Yield line mechanism adopted for the prediction of the ultimate load capacity.

455

	Maximum load [kN]		
	Exp.	Predicted	Design load

		Average	Characteristic	[kN]
SFRC	232/243	234	155	81
R/C	363/375	268	228	
R/FRC	512/477	467	397	265

456

457 Table 2 – Ultimate loads of investigated slabs: experimental, predicted and design values.

458

459 6. CONCLUSIONS

460 In the present study the effect of application of steel fibres in a slab element with a statically
461 redundant structural configuration under biaxial bending was investigated. Six concrete
462 2000×2000×150 mm solid slabs were tested under a concentrated load applied in the centre and
463 measurements were carried out on deflection and cracking behaviour. Two slabs were reinforced
464 with only steel fibres, two were reinforced with rebars and the last two slabs were reinforced with
465 both the rebars and the steel fibres. The main conclusions derived from the present work are as
466 follows.

- 467 - Utilization of 35 kg/m³ of steel fibres for the SFRC slabs, and 35 kg/m³ of reinforcing bars
468 in each direction for the R/C slabs, allowed to make a comparison between the efficiency of
469 the reinforcing solutions. Half the weight of steel in the SFRC slabs as compared to the R/C
470 ones, led to a peak load that was 64% of that obtained in the R/C specimens. The 3D
471 distribution of fibres seems to be able to guarantee higher efficiency in terms of load bearing
472 capacity in comparison with conventional rebars.
- 473 - SFRC slabs show limited ductility with respect to other reinforcing solutions. The lower
474 ductility in the SFRC slabs may also affect the maximum load that is reached in these
475 elements considering that the softening phase occurs before the appearance of negative

476 moment cracks when a flexible constraint is considered. Provision of rebars is suggested to
477 increase the deformation capacity of slabs.

478 - There is a positive interaction between steel fibres and reinforcing steel. In the R/FRC slabs,
479 while the rebars guarantee the ductile behaviour of the slabs, the steel fibres remain active
480 even under high levels of deflection giving their contribution also along the negative
481 moment crack as assumed in the limit analysis. In this case the choice of the ultimate crack
482 opening, set equal to 2.5 mm, allows to take into account the not contemporary contribution
483 of positive and negative bending moment acting respectively on the radial and
484 circumferential cracks.

485 Other observations made from the experiments and the prediction of the ultimate load based on
486 the MC 2010 approach are as comes in the following lines:

487 - stress-CMOD results obtained from the notched specimens show that while over time the
488 residual tensile strength values in a range of CMODs that correspond to SLS improve, the
489 residual strength for wider CMODs almost remains unchanged. This phenomenon may lead
490 to a reduction of the ductility of SFRC structural elements that needs to be considered and
491 further studied.

492 - Steel fibres are very effective in controlling deflection and cracking specifically in the SLS
493 behaviour. In the range between 120 kN and 200 kN, the R/FRC slabs show 75% to 100%
494 less deflection compared to the R/C specimens.

495 - A comparison between the negative moment cracks on the R/C and R/FRC slabs, shows that
496 steel fibres can play a major role in reducing crack openings in the absence of a
497 reinforcement layer on the top of the slabs.

498 - Following the approach suggested in *fib* MC 2010, and with the choice of the characteristic
499 length equal to the depth of the slab, the ultimate load bearing capacity of the slabs is
500 satisfactorily predicted by implementing a limit state analysis. The need of a redundancy

501 factor as suggested by the Model Code for SFRC contribution is also proved in case of
502 SFRC slabs.

503 - In order to apply a limit state analysis to FRC elevated slabs characterized by a 3c class at
504 28 days, one should be assured about the possibility of the formation of the expected failure
505 mechanism. Lower ductility of SFRC slabs without any rebars might not allow the complete
506 formation of the expected kinematic failure mechanism which could lead to unsafe
507 prediction for the ultimate load.

508 **ACKNOWLEDGEMENT**

509 The authors express their gratitude to the financial support provided by Steriline, Magnetti
510 Building, and Finazzi Company and the technical support provided by DSC-Erba. The authors are
511 also grateful to the assistance of Mr. Andrea G. Stefanoni for his contribution in carrying out the
512 experiments.

513 **REFERENCES**

- 514 [1] J. P. Romualdi and G. B. Batson, "Behaviour of Reinforced Concrete Beams with Closely
515 Spaced Reinforcement," *ACI J. Proc.*, vol. 60, no. 6, pp. 775–790, 1963.
- 516 [2] S. Shah and B. Rangan, "Fibre reinforced concrete properties," *ACI J. Proc.*, no. 68, pp. 126–
517 137, 1971.
- 518 [3] P. Rossi and G. Chanvillard, *PRO 15: 5th RILEM Symposium on Fibre-Reinforced Concretes*
519 *(FRC)-BEFIB'2000*, vol. 15. RILEM Publications, 2000.
- 520 [4] M. di Prisco, R. Felicetti, and G. A. Plizzari, *PRO 039: 6th International RILEM Symposium*
521 *on Fibre-Reinforced Concretes BEFIB'2004*. RILEM Publications, 2004.
- 522 [5] R. Gettu, *PRO 060: 7th International RILEM Symposium on Fibre Reinforced Concrete:*
523 *Design and Applications- BEFIB'2008*. RILEM Publications, 2008.
- 524 [6] A. E. Naaman, "New fiber technology," *Concrete International*, 20 (7), pp. 57-62, 1998.
- 525 [7] K. Wang, D. C. Jansen, S. P. Shah, and A. F. Karr, "Permeability study of cracked concrete,"

- 526 *Cem. Concr. Res.*, vol. 27, no. 3, pp. 381–393, Mar. 1997.
- 527 [8] P. H. Bischoff, “Tension stiffening and cracking of steel fibre reinforced concrete,” *J. Mater.*
528 *Civ. Eng.*, vol. 15, no. 2, pp. 174–182, 2003.
- 529 [9] H. H. Abrishami and D. Mitchell, “Influence of steel fibres on tension stiffening,” *ACI*
530 *Struct. J.*, vol. 94, no. 6, pp. 769–776, 1997.
- 531 [10] G. Tiberti, F. Minelli, G. A. Plizzari, and F. J. Vecchio, “Influence of concrete strength on
532 crack development in SFRC members,” *Cem. Concr. Compos.*, vol. 45, pp. 176–185, 2014.
- 533 [11] J. R. Deluce, L. Seong-Cheol, and F. J. Vecchio, “Crack model for steel fibre-reinforced
534 concrete members containing conventional reinforcement,” *ACI Struct. J.*, vol. 111, no. 1, pp.
535 93–102, 2014.
- 536 [12] P. Heek and P. Mark, “Load-bearing capacities of SFRC elements accounting for tension
537 stiffening with modified moment-curvature relations,” pp. 301–310, 2014.
- 538 [13] A. Meda, F. Minelli, and G. A. Plizzari, “Flexural behaviour of R/C beams in fibre reinforced
539 concrete,” *Compos. Part B Eng.*, vol. 43, no. 8, pp. 2930–2937, 2012.
- 540 [14] B. H. Oh, “Flexural analysis of reinforced concrete beams containing steel fibres” *J. Struct.*
541 *Eng.*, vol. 118, no. 10, pp. 2821–2835, 1992.
- 542 [15] S. H. Alsayed, “Flexural deflection of reinforced fibrous concrete beams” *ACI Struct. J.*, vol.
543 90, no. 1, pp. 72–88, 1993.
- 544 [16] L. Vandewalle, “Cracking behaviour of concrete beams reinforced with a combination of
545 ordinary reinforcement and steel fibres,” *Mater. Struct.*, vol. 33, no. 3, pp. 164–170, 2000.
- 546 [17] K. H. Tan, P. Paramasivam, and K. C. Tan, “Cracking characteristics of reinforced steel fibre
547 concrete beams under short- and long-term loadings,” *Adv. Cem. Based Mater.*, vol. 2, no. 4,
548 pp. 127–137, 1995.
- 549 [18] H. C. Mertol, E. Baran, and H. J. Bello, “Flexural behaviour of lightly and heavily reinforced
550 steel fibre concrete beams,” *Constr. Build. Mater.*, vol. 98, pp. 185–193, Nov. 2015.
- 551 [19] P. Pujadas, A. Blanco, A. De La Fuente, and A. Aguado, “Cracking behaviour of FRC slabs

- 552 with traditional reinforcement,” *Mater. Struct. Constr.*, vol. 45, no. 5, pp. 707–725, 2012.
- 553 [20] A. L. Dossland, *Fibre Reinforcement in Load Carrying Concrete Structures*, no. February.
554 Trondheim, 2008.
- 555 [21] M. di Prisco, G. Plizzari, and L. Vandewalle, “Fibre reinforced concrete: new design
556 perspectives,” *Mater. Struct.*, vol. 42, no. 9, pp. 1261–1281, 2009.
- 557 [22] B. Mobasher and X. Destrée, “Report on Design and Construction of Steel Fibre-Reinforced
558 Concrete Elevated Slabs,” in *SP-274 Fibre reinforced self-consolidating concrete: research
559 and applications*, 2010.
- 560 [23] L. Facconi, F. Minelli, and G. Plizzari, “Steel fibre reinforced self-compacting concrete thin
561 slabs--Experimental study and verification against Model Code 2010 provisions,” *Eng.
562 Struct.*, vol. 122, pp. 226–237, 2016.
- 563 [24] D. Fall, J. Shu, R. Rempling, K. Lundgren, and K. Zandi, “Two-way slabs: Experimental
564 investigation of load redistributions in steel fibre reinforced concrete,” *Eng. Struct.*, vol. 80,
565 pp. 61–74, 2014.
- 566 [25] Fédération internationale du béton, *Model code 2010: final draft*. Lausanne, Switzerland:
567 International Federation for Structural Concrete (fib), 2013.
- 568 [26] J. R. Roesler, D. A. Lange, S. A. Altoubat, K.-A. Rieder, and G. R. Ulreich, “Fracture of
569 plain and fibre-reinforced concrete slabs under monotonic loading,” *J. Mater. Civ. Eng.*, vol.
570 16, no. 5, pp. 452–460, 2004.
- 571 [27] L. G. Sorelli, A. Meda, and G. A. Plizzari, “Steel fibre concrete slabs on ground: A structural
572 matter,” *ACI Struct. J.*, vol. 103, no. 4, pp. 551–558, 2006.
- 573 [28] H. Falkner and V. Henke, “Application of steel fibre concrete for underwater concrete slabs,”
574 *Cem. Concr. Compos.*, vol. 20, no. 5, pp. 377–385, 1998.
- 575 [29] X. Destrée and J. Mandl, “Steel fibre only reinforced concrete in free suspended elevated
576 slabs: Case studies, design assisted by testing route, comparison to the latest SFRC standard
577 documents,” *Tailor Made Concr. Struct.*, pp. 437–443, 2008.

- 578 [30] J. Hedebratt and J. Silfwerbrand, “Full-scale test of a pile supported steel fibre concrete
579 slab,” *Mater. Struct. Constr.*, vol. 47, no. 4, pp. 647–666, 2014.
- 580 [31] M. di Prisco, P. Martinelli, and B. Parmentier, “On the reliability of the design approach for
581 FRC structures according to fib Model Code 2010: the case of elevated slabs,” *Struct.*
582 *Concr.*, vol. 17, no. 4, pp. 588–602, 2016.
- 583 [32] B. Parmentier, P. Van Itterbeeck, and A. Skowron, “The flexural behaviour of SFRC flat
584 slabs : the Limelette full-scale experiments for supporting design model codes.,” 2014.
- 585 [33] M. di Prisco, F. Sibaud, C. Failla, P. Finazzi, A. Siboni, A. Bassani, G. Nava, M. Colombo,
586 “Innovative SFRC applications: an industrial building in Como”, *Proc. of Italian Concrete*
587 *Days*, June 14-15, Lecco, ISBN 978-88-99916-11-4, 2018.
- 588 [34] EN 14651: Test method for metallic fibreed concrete-Measuring the flexural tensile strength
589 (limit of proportionality (LOP), residual),” *Brussels Eur. Comm. Stand.*, 2005.
- 590 [35] A. Blanco, P. Pujadas, A. De La Fuente, S. H. P. Cavalaro, and A. Aguado, “Assessment of
591 the fibre orientation factor in SFRC slabs,” *Compos. Part B Eng.*, vol. 68, pp. 343–354, Jan.
592 2015.
- 593 [36] S. J. Barnett, J.-F. Lataste, T. Parry, S. G. Millard, and M. N. Soutsos, “Assessment of fibre
594 orientation in ultra high performance fibre reinforced concrete and its effect on flexural
595 strength,” *Mater. Struct.*, vol. 43, no. 7, pp. 1009–1023, 2010.
- 596 [37] P. Pujadas *et al.*, “Plastic fibres as the only reinforcement for flat suspended slabs:
597 Parametric study and design considerations,” *Constr. Build. Mater.*, vol. 70, pp. 88–96, 2014.
- 598 [38] B. Zhou and Y. Uchida, “Relationship between fibre orientation/distribution and post-
599 cracking behaviour in ultra-high-performance fibre-reinforced concrete (UHPFRC),” *Cem.*
600 *Concr. Compos.*, vol. 83, pp. 66–75, 2017.
- 601 [39] P. Soroushian and C. D. Lee, “Distribution and orientation of fibres in steel fibre reinforced
602 concrete,” *ACI Mater. J.*, vol. 87, no. 5, pp. 433–439, 1990.
- 603 [40] A. Neville, *Properties of concrete*. 1995.

- 604 [41] T. E. T. Buttignol, M. Colombo, and M. di Prisco, “Long-term aging effects on tensile
605 characterization of steel fibre reinforced concrete,” *Structural Concrete*, vol. 17, no. 6. pp.
606 1082–1093, 2016.
- 607 [42] R. Park and W. L. Gamble, *Reinforced concrete slabs*. John Wiley & Sons, 2000.
- 608 [43] M. Otieno, M. G. Alexander, and H.-D. Beushausen, “Corrosion in cracked and uncracked
609 concrete – influence of crack width, concrete quality and crack reopening,” *Mag. Concr.*
610 *Res.*, vol. 62, no. 6, pp. 393–404, 2010.
- 611 [44] J. Rapoport, C.-M. Aldea, S. P. Shah, B. Ankenman, and A. Karr, “Permeability of Cracked
612 Steel Fibre-Reinforced Concrete.”
- 613 [45] C. G. Berrocal, I. Löfgren, K. Lundgren, and L. Tang, “Corrosion initiation in cracked fibre
614 reinforced concrete: Influence of crack width, fibre type and loading conditions,” *Corros.*
615 *Sci.*, vol. 98, pp. 128–139, 2015.
- 616 [46] C. G. Berrocal, I. Löfgren, K. Lundgren, N. Görander, and C. Halldén, “Characterisation of
617 bending cracks in R/FRC using image analysis,” *Cem. Concr. Res.*, vol. 90, pp. 104–116,
618 2016.
- 619 [47] N. Banthia and R. Gupta, “Hybrid fibre reinforced concrete (HyFRC): fibre synergy in high
620 strength matrices,” 2004.
- 621 [48] S. H. Park, D. J. Kim, G. S. Ryu, and K. T. Koh, “Tensile behaviour of Ultra High
622 Performance Hybrid Fibre Reinforced Concrete,” *Cem. Concr. Compos.*, vol. 34, pp. 172–
623 184, 2012.
- 624 [49] D. J. Kim, S. H. Park, G. S. Ryu, and K. T. Koh, “Comparative flexural behaviour of Hybrid
625 Ultra High Performance Fibre Reinforced Concrete with different macro fibres,” *Constr.*
626 *Build. Mater.*, vol. 25, pp. 4144–4155, 2011.
- 627 [50] L. G. Sorelli, A. Meda, and G. A. Plizzari, “Bending and uniaxial tensile tests on concrete
628 reinforced with hybrid steel fibres,” *J. Mater. Civ. Eng.*, vol. 17, no. 5, pp. 519–527, 2005.
- 629 [51] H. Salehian, J. A. O. Barros, and M. Taheri, “Evaluation of the influence of post-cracking

- 630 response of steel fibre reinforced concrete (SFRC) on load carrying capacity of SFRC
631 panels,” *Constr. Build. Mater.*, vol. 73, pp. 289–304, 2014.
- 632 [52] C. Kleinman, X. Destrée, A. Lambrechts, and A. Hoekstra, “Steel Fibre As Only Reinforcing
633 in Free Suspended One Way Elevated Slabs : Design ConcluKleinman, C., Destrée, X.,
634 Lambrechts, A., & Hoekstra, A. (2012). Steel Fibre As Only Reinforcing in Free Suspended
635 One Way Elevated Slabs : Design Conclusions of a Tu,” pp. 1–13, 2012.
- 636 [53] M. Colombo, P. Martinelli, and M. di Prisco, “On the evaluation of the structural
637 redistribution factor in FRC design: a yield line approach,” *Mater. Struct.*, vol. 50, no. 1, p.
638 100, 2017.
- 639